

Received October 30, 2018, accepted November 20, 2018, date of publication November 28, 2018, date of current version December 27, 2018.

Digital Object Identifier 10.1109/ACCESS.2018.2883757

# Multidirectional Alternating Current Potential Drop Technique for Detecting Random Cracks

WENYANG LI<sup>1</sup>, FANGJI GAN<sup>1</sup>, SHIPING ZHAO<sup>1</sup>, YONGJIE ZHOU<sup>2</sup>, AND XIAOMING HE<sup>2</sup>

<sup>1</sup>School of Manufacturing Science and Engineering, Sichuan University, Chengdu 610065, China

<sup>2</sup>College of Physics and Electronic Information Engineering, Qinghai Normal University, Xining 810016, China

Corresponding author: Fangji Gan (gfj0318@foxmail.com)

This work was supported in part by the National Natural Science Foundation of China under Grant 51704199 and in part by the Natural Science Foundation of Qinghai Province under Grant 2018-ZJ-719.

**ABSTRACT** The alternating current potential drop technique has been widely used to measure subsurface cracks in metal structures. However, the application of the technique to random cracks has, to date, been limited. By using a multidirectional alternating current potential drop technique, the angle between crack and exciting electrode wire changes from 0° – 90° to 67.5° – 90°, which considerably expanded the ranges of detection. Simulation and experiment results showed that this technique can accurately measure the depth of random cracks.

**INDEX TERMS** Alternating current potential drop technique, multidirectional current, random cracks, depth measurement.

## I. INTRODUCTION

The alternating current potential drop (ACPD) technique makes use of an increase in electrical resistance of a metallic conductor caused by crack initiation and growth [1]. It can achieve high sensitivity with low injected current [2]–[4]. The technique is based on ‘skin effect’ [5]–[8], which is closely related to the current frequency. As the frequency decreases, the current distribution in the material shifts from the surface of the conductor to the entire conductor. The skin depth  $\delta$  can be represented by the following relation:

$$\delta = \frac{1}{\sqrt{\pi \mu_r \mu_0 \sigma f}} \quad (1)$$

where  $\mu_r$  is the relative magnetic permeability,  $\mu_0$  the magnetic permeability of free space,  $\sigma$  the electrical conductivity, and  $f$  the frequency of excitation current.

Figure 1(a) shows the initial state of a metal pipe without defects. After a period of service, defects form in the inner walls of the pipe, whereas the outer walls are always well protected. Figure 1(b) shows a crack defect with depth  $d$  in the inner wall.

$I(f)$  is the excitation current with frequency  $f$ . It can be represented by:

$$I(f) = Ie^{j2\pi ft} \quad (2)$$

Where  $I$  is the current amplitude,  $j = \sqrt{-1}$ , and  $t$  is time.

The electric field equation is as follows:

$$\nabla^2 E(r) + k^2 E(r) = 0 \quad (3)$$

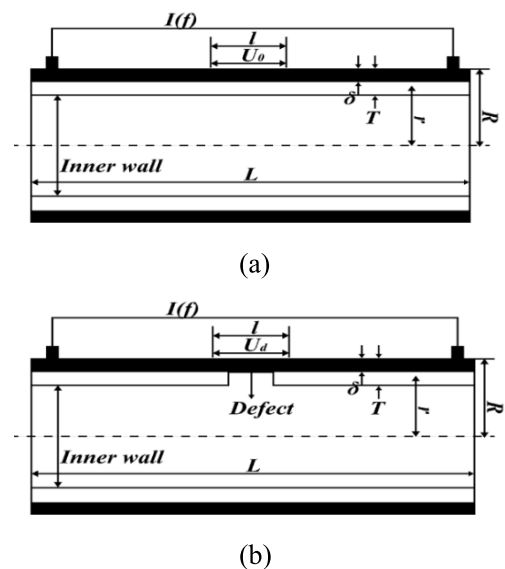


**FIGURE 1.** Schematic diagram of (a) initial state without defects and (b) presence of a crack defect.

with

$$k = (1 - j)\sqrt{\pi \mu_r \mu_0 \sigma f} \quad (4)$$

The current density  $J(r)$  can be determined by the intensity of the electric field at the same position  $r$ :

$$J(r) = \sigma E(r) \quad (5)$$

Where  $r$  is the radial position measured from the center of the conductor, and  $E(r)$  is the intensity of the electric field at  $r$ .

The solution of  $J(r)$  in the conductor is as follows [9]:

$$J(r) = \frac{Ik}{2\pi R} \cdot \frac{J_0(kr)}{J_1(kR)} \quad (6)$$

where  $J_0$  and  $J_1$  are Bessel functions of the first kind, with order zero and one, respectively,  $R$  is the outer radius of specimen, and  $l$  is the distance between each pair of electrodes, so the theoretical potential drop across this distance can be described as:

$$U(r) = l \cdot \frac{I \cdot k}{2\pi R\sigma} \cdot \frac{J_0(kr)}{J_1(kR)} \quad (7)$$

Bessel functions can be approximated by an exponential function. In this case, the absolute value of the voltage can be written as [10]:

$$|U(r)| = \frac{I}{\sqrt{2\pi R\delta}} e^{-\frac{r-R}{\delta}} \quad (8)$$

Equation (8) shows that the voltage changes at different radial distances. In this work, the contact depth  $d_0$  between the potential electrodes and the outer wall of the pipe was approximately 0.5mm, so the voltage obtained on the two electrodes was:

$$U = \frac{I}{\sqrt{2\pi R\delta}} e^{-\frac{d_0}{\delta}} \quad (9)$$

The wall thickness of the pipe is given by  $T$ . The initial voltage is  $U_0$ , and the voltage measured with a defect is  $U_d$ . An approximation can be made using (9). If the defect of the inner wall is extremely shallow ( $d \approx 0$ ), then, as the frequency decreases,  $U_d/U_0$  approaches 1. If the defect of the inner wall is attributed to general corrosion [11], [12], then, as the frequency decreases,  $U_d$  remains constant once  $\delta = T - d$ , and  $U_d/U_0 \approx m/U_0$  (where  $m$  is constant). However, if the defect is a crack, the current around the defect layer will infiltrate downward as the frequency decreases, i.e.,  $U_d < m$ , then  $U_d/U_0 < m/U_0$ .

Therefore, a general solution to calculate a crack defect can be approximated by a linear superimposition of two extreme cases: that without defects and that where the defect is due to general corrosion:

$$\frac{U_d}{U_0} = a_1 \cdot 1 + a_2 \cdot de^{a_3d} \quad (10)$$

where  $a_1$ ,  $a_2$  and  $a_3$  are constants.

## II. MULTIDIRECTIONAL ACPD TECHNOLOGY DEVELOPMENT

We studied the relationship between the directions of the exciting electrode wire and the crack. The COMSOL finite element simulation software (COMSOL Inc., Stockholm, Sweden) was used to perform a numerical analysis to illustrate the relationship. Figure 1 shows the metal pipe simulation model with properties as listed in Table 1.

TABLE 1. Parameters of model.

V/A	$\sigma$ /ms	$\mu_r$	l/mm	R~r~L/mm	T/mm	d/mm
2	43	1	20	160~140~400	10	2~0.5~6

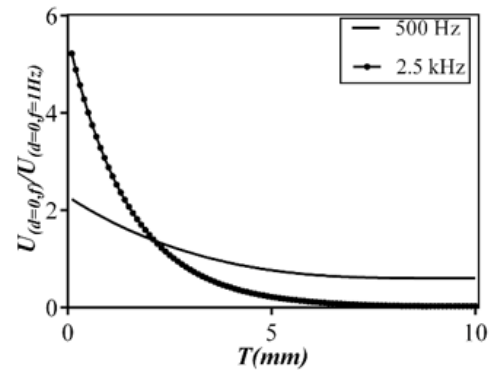


FIGURE 2. Calculated distribution of alternating current potential drop.

The calculated distribution of potential drop was obtained by substituting parameters from Table 1 and current frequency  $f$  into (4) and (7).

Before calculating the potential drop, we should confirm the value of  $f$ . In Figure 2, the skin current could not completely penetrate the pipe wall at 2.5 kHz, so the voltage  $U_d$  could not reflect information pertaining to a shallow defect in this case. When the frequency decreased to 500 Hz, the penetration current was able to reach the defect layer at each depth. Considering that  $\delta$  should be smaller than the wall thickness ( $T = 10$  mm), the lower limit of frequency was calculated as 59 Hz according to (1). Therefore, the current frequency could be selected between 59 and 500 Hz. In this work, we chose 100 Hz as the frequency of the excitation current.

In Figure 3(a),  $U_0$  could be obtained without defects. Figures 3(b)-(e) represented four position defects with the same length, width, and depth.  $\varphi$  is the angle between the crack and exciting electrode wire.

In Figure 5, when  $\varphi$  was smaller than  $45^\circ$ , the value of  $U_d/U_0$  could not assess the crack depth using (10). However, when  $\varphi$  was greater than  $45^\circ$ , and the closer it was to  $90^\circ$ , the more closely the relationship between the value of  $U_d/U_0$  and crack depth followed the exponential distribution of (10). In addition, the value of  $U_d/U_0$  at  $90^\circ$  was larger than at any other angle.

The variation of  $U_d$  could be assessed by Ohm' law. We could regard the area measured between the potential electrodes as a volume resistance  $R_{es}$ .

$$U_d = R_{es}I \quad (11)$$

$R_{es}$  was conversed with the cross-section of the volume resistance:

$$R_{es} = \frac{\rho l}{S} \propto \frac{1}{S} \quad (12)$$

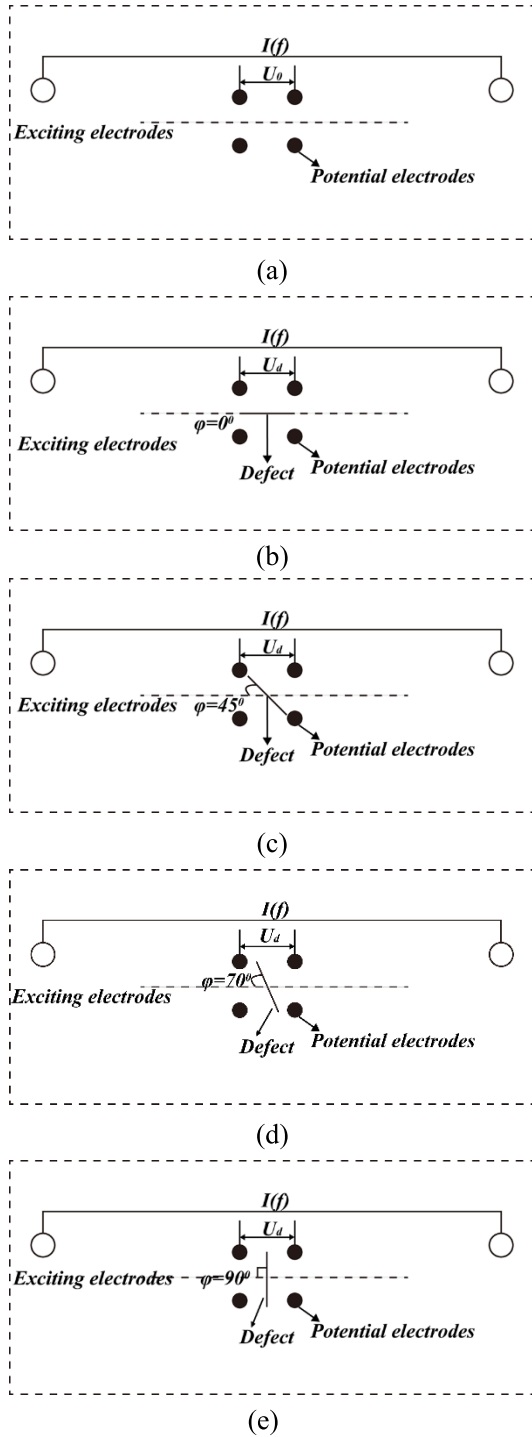


**FIGURE 3.** Diagrams of (a) initial state without defects and with crack defects at (b) 0°, (c) 45°, (d) 70°, and (e) 90° relative to the position of the electrode wire.

Where  $\rho$  is the resistivity of conductor, and  $S$  is the cross-section perpendicular to the direction of the current.

Figures 4(a)-(b) represented the current distribution of two cases involved in Figure 3, where  $\varphi$  were 0° and 90°. Compared Figure 4(a) with 4(b), the current flew through a larger cross-section when  $\varphi$  was 0°:

$$S_1 > S_4 \tag{13}$$

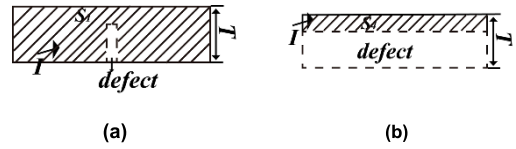


**FIGURE 4.** current distribution in the cross sectional area of two cases ( $\varphi = 0^\circ, 90^\circ$ ).

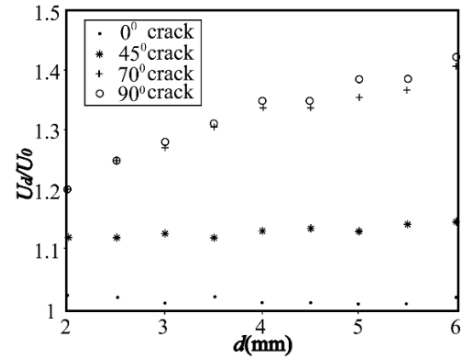


**FIGURE 5.** Voltage ratio curve ( $\varphi = 0^\circ, 45^\circ, 70^\circ, 90^\circ$ ).

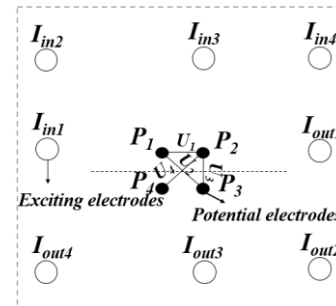


**FIGURE 6.** Measured metal with multidirectional current ( $U_1$  represents  $U_{1d}$  or  $U_{10}$ ,  $U_2$  represents  $U_{2d}$  or  $U_{20}$ ,  $U_3$  represents  $U_{3d}$  or  $U_{30}$ ,  $U_4$  represents  $U_{4d}$  or  $U_{40}$ ).

Where  $S_1$  is the cross-section of 0° crack, and  $S_4$  is of 90° crack.

Substituting (13) into (12), We could observe that the value of  $R_{es}$  at 0° was smaller than 90°. Thus the former voltage was smaller than the latter. A method defined as the multidirectional alternating current potential drop (MACPD) technique was therefore extracted to measure random crack depths. The angle between the crack and exciting electrode wire changed from 0° -90° to 67.5° -90° by adding three sets of excitation currents, as shown in Figure 6.

The depth could be accurately determined by substituting the largest values of  $U_d/U_0$  from the four voltages as follows into (10):

$$\left( \frac{U_{1d}}{U_{10}}, \frac{U_{2d}}{U_{20}}, \frac{U_{3d}}{U_{30}}, \frac{U_{4d}}{U_{40}} \right)$$

### III. EXPERIMENTAL VERIFICATION

To verify the accuracy of the proposed method, experiments were conducted using an SR850 digital lock-in amplifier (Stanford Research Systems, CA, USA) and a power ampli-

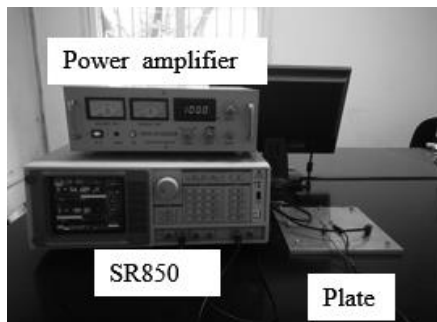


FIGURE 7. Experimental equipment.

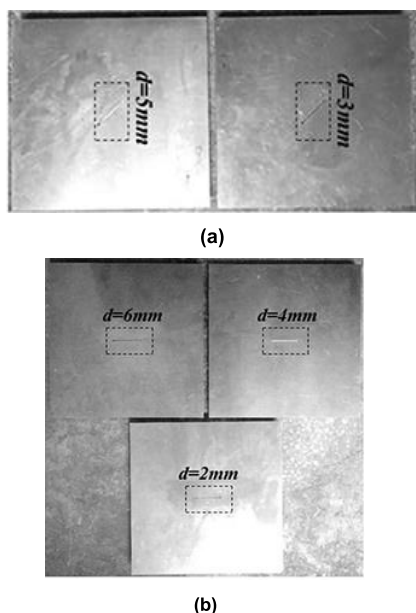


FIGURE 8. Metal plate specimens with crack defects at (a) 45° and (b) 0°.

fier, as shown in Figure 7. The power amplifier provided a maximum sinusoidal current ( $I$ ) of 2 A with a frequency at 100 Hz from a source signal from the SR850 amplifier. Figure 6 shows the probe configuration. Five 220 mm × 220 mm × 10 mm metal plates were used as test specimens, as shown in Figure 8. The  $\mu_r$ ,  $\mu_0$ , and  $\sigma$  values of these specimens are summarized in Table 1. Plate 1-2 measured cracks at 45° at depths of 3 mm and 5 mm. Plate 3-5 had 0° cracks at depths of 2 mm, 4 mm, and 6 mm.

Before machining the defects, alternating current of 2 A with a frequency of 100 Hz was successively injected into the plate through  $I_{in1}$ ,  $I_{in2}$ ,  $I_{in3}$ , and  $I_{in4}$ . The SR850 amplifier was used to measure the initial voltages  $U_{10}$ ,  $U_{20}$ ,  $U_{30}$ , and  $U_{40}$  between probes ( $P_1-P_2$ ), ( $P_1-P_3$ ), ( $P_2-P_3$ ), and ( $P_3-P_4$ ), respectively. The values of  $U_{1d}$ ,  $U_{2d}$ ,  $U_{3d}$ , and  $U_{4d}$  were obtained in the same way.

After the voltage measurements were completed, eight voltages for each plate were obtained. Substituting the largest values of  $U_d/U_0$  into (10), we could acquire the results. The constants in (10) were given by simulation data. COMSOL

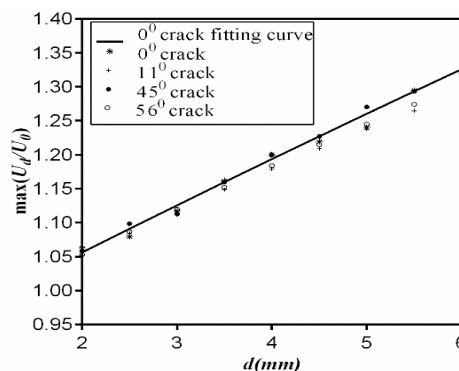


FIGURE 9.  $\text{Max}(U_d/U_0)$ - $d$  curve( $\varphi = 0^\circ$ ).

TABLE 2. Simulation results.

$\varphi$	Real depth (mm)	Measuring depth (mm)	error (%)
0	2.00	1.93	-0.7
	3.00	2.86	-1.4
	4.00	3.79	-2.1
	5.00	4.65	-3.5
	6.00	5.51	-4.9
45	2.00	2.03	0.3
	3.00	2.81	-1.9
	4.00	4.15	1.5
	5.00	5.15	1.5
	6.00	6.17	1.7
56	2.00	1.96	-0.4
	3.00	2.91	-0.9
	4.00	3.79	-2.1
	5.00	4.77	-2.3
	6.00	5.64	-3.6

Multiphysics 4.5 was used for theoretical calculations. Material parameters and dimensions of the simulation model were the same as test specimens. The simulation cracks measured at 0°, 11°, 45°, and 56° at depths of 2 mm, 2.5 mm, 3 mm, 3.5 mm, 4 mm, 4.5 mm, 5 mm, 5.5 mm and 6 mm. Figure 9 and (14) showed the fitting results. Table 2 showed the partial results of simulation. The measuring depth could be obtained by substituting the largest values of  $U_d/U_0$  into (14). The error was calculated by [14], [15]:

$$\text{error} (\%) = 100 \% \times (\text{measuring depth} - \text{Real depth})/T$$

$$\frac{U_d}{U_0} = 0.9137 + 0.07261de^{-0.009146d} \quad (14)$$

Table 3 showed the voltage ratios of different depths and angles based on 5 test specimens. The results were listed in Table 4.

**TABLE 3. The voltage ratio of different depths and directions.**

$\varphi^0$	$d/mm$	$\frac{U_1(d)}{U_{10}}$	$\frac{U_2(d)}{U_{20}}$	$\frac{U_3(d)}{U_{30}}$	$\frac{U_4(d)}{U_{40}}$
0	2.00	0.950	0.956	1.091	0.988
	4.00	0.967	1.086	1.191	1.048
	6.00	0.952	1.236	1.350	1.237
45	3.00	0.992	0.952	1.003	1.142
	5.00	1.044	0.987	1.055	1.269

**TABLE 4. Experimental results.**

$\varphi^0$	Real depth (mm)	Measuring depth (mm)	error (%)
0	2.00	2.49	4.9
	4.00	3.96	-0.4
	6.00	6.37	3.7
45	3.00	3.24	2.4
	5.00	5.15	1.5

The results clearly demonstrated that the proposed method could accurately measure the depth of random crack defects.

#### IV. CONCLUSION

MACPD could be used to assess random defects on a subsurface. We used the largest values of  $U_d/U_0$  to determine the crack depth because numerical analysis showed that the angle between the crack and exciting electrode wire changed from  $0^\circ$ – $90^\circ$  to  $67.5^\circ$ – $90^\circ$  by using this technique. The experimental results were in good agreement with fitted equations based on simulation.

To enable the more widespread use of MACPD technology, the applicability of (14) to identifying cracks with varying depth and the occurrence of complex defects (cracks) should also be considered.

#### REFERENCES

- [1] G. Sposito, P. Cawley, and P. B. Nagy, "Potential drop mapping for the monitoring of corrosion or erosion," *NDT&E Int.*, vol. 43, pp. 394–402, Jul. 2010.
- [2] H. Saguy and D. Rittel, "Application of AC tomography to crack identification," *Appl. Phys. Lett.*, vol. 91, p. 084104, Aug. 2007.
- [3] J. R. Bowler, Y. Huang, H. Sun, J. Brown, and N. Bowler, "Alternating current potential-drop measurement of the depth of case hardening in steel rods," *Meas. Sci. Technol.*, vol. 19, p. 075204, Jun. 2008.
- [4] J. R. Bowler and N. Bowler, "Theory of four-point alternating current potential drop measurements on conductive plates," *Proc. Roy. Soc. A, Math., Phys. Eng. Sci.*, vol. 463, pp. 817–836, Mar. 2007.
- [5] Y. Li, F. Gan, Z. Wan, J. Liao, and W. Li, "Novel method for sizing metallic bottom crack depth using multi-frequency alternating current potential drop technique," *Meas. Sci. Rev.*, vol. 15, p. 268, Oct. 2015.
- [6] Y. Li, F. Gan, Z. Wan, and J. Liao, "An SVM approach with alternating current potential drop technique to classify pits and cracks on the bottom of a metal plate," *AIP Adv.*, vol. 6, p. 095202, Sep. 2016.
- [7] H. Saguy and D. Rittel, "Alternating current flow in internally flawed conductors: A tomographic analysis," *Appl. Phys. Lett.*, vol. 89, p. 094102, Aug. 2006.
- [8] H. Saguy and D. Rittel, "Flaw detection in metals by the ACPD technique: Theory and experiments," *NDT&E Int.*, vol. 40, pp. 505–509, Oct. 2007.
- [9] I. Verpoest, E. Aernoudt, A. Deruyttere, and M. Neyrinck, "An improved A.C. potential drop method for detecting surface microcracks during fatigue tests of unnotched specimens," *Fatigue Eng. Mater. Struct.*, vol. 3, pp. 203–217, Jul. 2007.
- [10] I. S. Hwang, "A multi-frequency AC potential drop technique for the detection of small cracks," *Meas. Sci. Technol.*, vol. 3, p. 62, Jan. 1999.
- [11] D. Rujiao, H. Renyang, and Y. Yong, "Research progress on new technology of pipeline non-destructive corrosion monitoring," *Pipeline Technol. Equip.*, vol. 6, pp. 18–20, Jun. 2014.
- [12] D. R. Clarida, R. J. Scanlan, and R. M. Boothman, "Corrosion monitoring experience in the refining industry using the FSM technique," *NACE Int.*, vol. 3, pp. 16–20, Mar. 2003.
- [13] K. Ikeda, M. Yoshimi, and C. Miki, "Electrical potential drop method for evaluating crack depth," *Int. J. Fract.*, vol. 47, pp. 25–38, Jan. 1991.
- [14] F. Gan, Z. Wan, Y. Li, J. Liao, and W. Li, "Improved formula for localized corrosion using field signature method," *Measurement*, vol. 63, pp. 137–142, Mar. 2014.
- [15] F. Gan, G. Tan, Z. Wan, J. Liao, and W. Li, "Investigation of pitting corrosion monitoring using field signature method," *Measurement*, vol. 82, pp. 46–54, Mar. 2016.
- [16] Z.-J. Lu, P. J. Nicholas, and W. J. Evans, "Calibration of an ACPD monitoring system for small crack growth in corner crack specimens," *Eng. Fract. Mech.*, vol. 50, pp. 443–456, Mar. 1995.
- [17] J. Y. Yoon et al., "On-line monitoring of environment-assisted cracking in nuclear piping using array probe direct current potential drop," *J. Nondestruct. Eval.*, vol. 35, p. 13, Mar. 2016.
- [18] T. V. Venkatsubramanian and B. A. Unvala, "An AC potential drop system for monitoring crack length," *J. Phys. E, Sci. Instrum.*, vol. 17, p. 765, Sep. 1984.
- [19] R. D. Strømmen, H. Horn, and G. Moldestad, "FSM—Non-intrusive monitoring of internal corrosion, erosion and cracking," *Anti-Corrosion Methods Mater.*, vol. 42, pp. 3–6, Jun. 1995.
- [20] N. Merah, "Detecting and measuring flaws using electric potential techniques," *J. Qual. Maintenance Eng.*, vol. 9, pp. 160–175, Feb. 2003.
- [21] G. Sposito, P. Cawley, and P. B. Nagy, "An approximate model for three-dimensional alternating current potential drop analyses using a commercial finite element code," *NDT&E Int.*, vol. 43, pp. 134–140, Mar. 2010.
- [22] D. Mirshekar-Syahkal, R. Collins, and D. H. Michael, "The influence of skin depth on crack measurement by the AC field technique," *J. Nondestruct. Eval.*, vol. 3, pp. 65–76, Jun. 1982.
- [23] D. Mirshekar-Syahkal, "Probe characterization in AC field measurements of surface crack depth," *J. Nondestruct. Eval.*, vol. 3, pp. 9–17, Mar. 1982.
- [24] Y. Feng, L. Zhang, and W. Zheng, "Simulation analysis and experimental study of an alternating current field measurement probe for pipeline inner inspection," *NDT&E Int.*, vol. 98, pp. 123–129, Sep. 2018.
- [25] C. Jiapeng, "Quantitative analysis of skin effect," *Phys. Eng.*, vol. 2, pp. 7–10, Feb. 1988.
- [26] L. Chuangao and D. Yixiong, "Accurate measuring of crack—Depth," *Electr. Locomotives Transit Vehicles*, vol. 33, pp. 43–46, Sep. 2010.
- [27] G. Songhua, "The magnetic and electric field produced by alternating current in a long solenoid," *Phys. Eng.*, vol. 13, pp. 6–8, Jul. 2003.
- [28] W. D. Dover and C. C. Monahan, "The measurement of surface breaking cracks by the electrical systems ACPD/ACFM," *Fatigue Fract. Eng. Mater. Struct.*, vol. 17, pp. 1485–1492, Dec. 1994.
- [29] D. H. Michael, R. T. Waechter, and R. Collins, "The measurement of surface cracks in metals by using A.C. electric fields," *Proc. Roy. Soc. A, Math. Phys. Eng. Sci.*, vol. 381, pp. 139–157, Aug. 1982.
- [30] N. Bowler, "Four-point potential drop measurements for materials characterization," *Meas. Sci. Technol.*, vol. 22, p. 012001, Nov. 2010.
- [31] M. K. Raja, S. Mahadevan, B. P. C. Rao, S. P. Behera, T. Jayakumar, and B. Raj, "Influence of crack length on crack depth measurement by an alternating current potential drop technique," *Meas. Sci. Technol.*, vol. 21, p. 105702, Aug. 2010.



**WENYANG LI** received the B.S. degree in measurement and control technology and instrument from Sichuan University, China, in 2017, where she is currently pursuing the Ph.D. Her area of research is non-destructive testing technology.



**FANGJI GAN** received the B.S. degree in measurement and control technology and instrument and the Ph.D. degree in test metrology technology and instrument from Sichuan University, China, in 2011 and 2016, respectively. Since 2016, he has been with the School of Manufacturing Science and Engineering, Sichuan University. From 2016 to 2018, he was an Assistant Research Fellow. Since 2018, he has been an Associate Research Fellow. His research interests include structural health monitoring, nondestructive testing, machine vision, and electromagnetic detection technology.



**SHIPING ZHAO** received the B.S. degree from Chengdu Science and Technology University in 1982 and the M.S. and Ph.D. degrees from Chongqing University, Chongqing, China, in 1986 and 1991, respectively, all in precision instrument. He is currently a Professor with the Instrument Science and Technology, Sichuan University, China. He was involved in mechatronics system and control technology and nondestructive testing.



**YONGJIE ZHOU** received the B.S. degree in physical sciences from Lanzhou City University, Lanzhou, China, in 2011, and the M.S. degree in plasma physics from Northwest Normal University, Lanzhou, in 2014. He is currently pursuing the Ph.D. degree in computer science with Qinghai Normal University, Xining, China. Since 2014, he has been a Lecturer with Physics and Electronic Engineering Department, Northwest Normal University. His research interests include the low temperature plasma discharges processes and applications, discharge in liquids, spectroscopic diagnostics, and algorithm analysis.



**XIAOMING HE** received the B.S. degree in physical sciences from Beijing Normal University, Beijing, China, in 1986. Since 1986, she has been with Physics and Electronic Engineering Department, Northwest Normal University, Xining, China. From 1986 to 2000, she was a Lecturer. From 2000 to 2008, she was an Assistant Professor. Since 2008, she has been a Professor. Her research interests include the physical properties of high temperature superconducting, algorithm analysis, and nondestructive testing.

...